Kinetics of Thermally Induced Phase Separation in a Crystallizable Polymer Solution

P. D. Graham and A. J. McHugh*

Department of Chemical Engineering, University of Illinois, 600 S. Mathews Avenue, Urbana, Illinois 61801

Received July 15, 1997; Revised Manuscript Received November 5, 1997

ABSTRACT: Small angle light scattering, differential scanning calorimetry, and electron microscopy have been used to quantify the kinetics of liquid−liquid phase separation and crystallization during thermal quenching of a polyethylene copolymer in anisole solution. Measurements of the time dependence of the position of the light scattering maximum were made following temperature quenching to various regions of the phase diagram. For quenches to temperatures above the crystallization temperature, domain growth rates increase with increasing quench depth and decreasing overall polymer concentration. Light scattering and microscopy show that solutions quenched to regions below the crystallization temperature show a brief coarsening period before structure growth is arrested by crystallization. Simultaneous measurement of the transient solution temperature indicates that cessation of domain growth occurs when the solution temperature crosses the crystallization line.

Introduction

Thermal induced phase separation (TIPS) of polymer solutions is an important processing technique used in the fabrication of microcellular foams[1] and microporous membranes.[2−5] In this process, liquid demixing, induced by thermal quenching, results in a two-phase structure consisting of a polymer-rich matrix surrounding polymer-lean droplets. The droplets continue to coarsen until their growth is arrested by solidification of the polymer-rich phase via either gelation,[6] glass transition,[7] or crystallization.[8,9] The latter step is critical since it freezes in the nonequilibrium morphology that eventually serves as the final product.

Because of their ability to withstand high temperatures, semicrystalline polymers are often used in the TIPS process.[10] In these systems, liquid−liquid or crystal−liquid phase separation may occur separately, or depending on the location in the phase diagram, both transitions may occur simultaneously. In the latter case, the relative phase transition rates apparently determine whether a porous liquid−liquid morphology will be locked-in by crystallization. Richards[11] was probably the first to show that the thermodynamic phase diagram for polyethylene exhibits both liquid−liquid phase separation and crystallization regions in a number of poor solvents. Similar behavior has since been reported for other crystallizable systems, including hydrogenated polybutadiene,[9] poly(vinyl chloride),[12] poly(vinyl alcohol),[13] and isotactic polypropylene.[8,10] In a number of studies of these systems, real space microscopy has been used to provide evidence for the role of the phase separation and crystallization kinetics on the morphology development.[8,9,10,14]

Our recent study of amorphous PMMA solutions[7] has shown that small angle light scattering can be a very useful technique for monitoring in situ the liquid-phase transition kinetics and its arrest due to a glass transition. In this paper we wish to show the applicability of the same technique to a crystallizable system, thereby allowing quantification of the interplay between liquid−liquid phase separation and its arrest due to crystallization. Measurements were made on solutions of a polyethylene copolymer in anisole which were quenched to different regions of the phase diagram, above and below the crystallization temperature.

Experimental Section

Materials and Methods. The polymer, poly(ethylene-*co*-methyl acrylate-*co*-acrylic acid) (6.5 wt % methyl acrylate, 6.5 wt % acrylic acid) (Aldrich), and the solvent (reagent grade anisole (Aldrich)) were used as received. Cloud points were determined by measuring light transmission of slow-cooled (0.5 °C/min) solutions in rectangular glass cells (path length 0.4 cm). The cloud point was taken as the temperature at which transmitted light intensity began to sharply decrease.

Crystallization experiments were performed on a Perkin-Elmer DSC 7. Samples were fully homogenized in sealed glass test tubes before being transferred into volatile sample pans. Exact compositions were determined by puncturing the pans after the experiment, heating them to above the melting temperature, and measuring the mass loss on vacuum-drying to constant weight.

The small angle light scattering (SALS) apparatus used for the quenching experiments is the same as that described in our earlier study.[7] Solutions were enclosed in a rectangular glass cell of path length ca. 0.05 cm and placed into a thermostated water bath at the desired phase separation temperature. Small angle scattering patterns from the sample were video recorded and digitized using a frame grabber. In all cases, the data to be shown are based on an average of several runs. Solution temperatures during the transient quench period were also separately monitored using a thermocouple sandwiched between two glass plates containing the solution. Figure 1 shows data for the solution temperature for runs made at three different quench temperatures. In most cases, thermal equilibration of the solution occurred on the order of 20 s, while data (to be shown) indicate that the late stages of liquid−liquid growth occur on time scales much greater than this.

Morphologies of several of the quenched films were also determined using scanning electron microscopy (SEM). Following removal from the glass cells, the samples were immersed in isopropyl alcohol to extract the anisole and then vacuum-dried for at least 24 h. Samples were freeze-fractured in liquid nitrogen and sputter coated (Emscope SC400 Sputter coater), for imaging on an Hitachi S-530 scanning electron microscope.

S0024-9297(97)01056-5 CCC: $15.00
Published on Web 03/24/1998

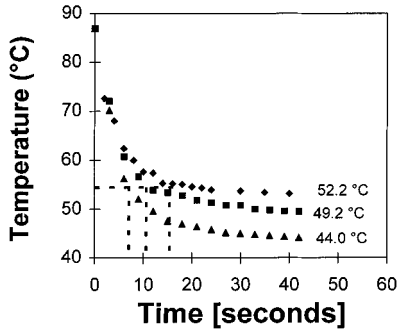

Figure 1. Transient solution temperatures measured in situ following quenches to temperatures indicated.

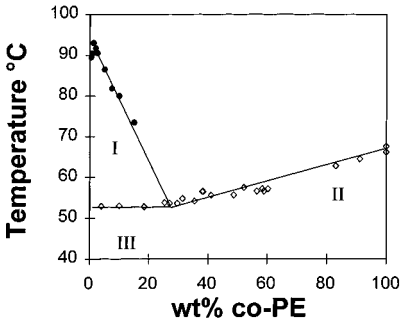

Figure 2. Cloud point curve (●) and crystallization temperatures (◇) for the co-PE/anisole system. Region I corresponds to the liquid−liquid equilibrium, II corresponds to the crystalline−liquid equilibrium, and III corresponds to the coexistence of two liquid and one crystalline phase.

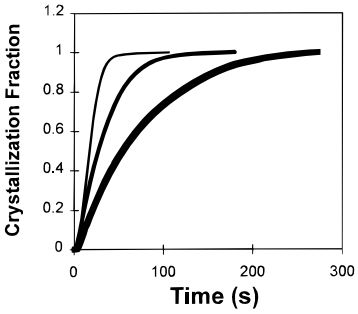

Figure 3. Time dependence of the fractional crystallization for 10 wt % co-PE/anisole solution quenched to three temperatures; (thin line) 47 °C; (medium line) 49 °C; (thick line) 51 °C.

Results and Discussion

Phase Diagram. Figure 2 shows the cloud point and crystallization curves for our poly(ethylene-*co*-methyl acrylate-*co*-acrylic acid) (co-PE)/anisole system. Regions I, II, and III denote, respectively, liquid−liquid phase equilibrium, liquid−crystal equilibrium, and three-phase liquid−liquid−crystal equilibrium. The characteristics shown here are typical of other crystallizable polymer/poor solvent systems.[9,15,16] In our case, crystallization temperatures were conveniently determined by cooling solutions in the DSC at 10 °C/min and noting the temperature at which the thermogram first deviated from the baseline value. A number of DSC runs showed that rapid quenches to the same temperatures, followed by continuous monitoring of the heat flux, gave the same results. Figure 3 shows an example of the fractional crystallization based on such runs for a 10 wt % co-PE/anisole solution. The trend of increasing crystallization rate with increasing quench depth results from both increased supercooling and an increase in the polymer concentration in the polymer-rich phase that forms. These data indicate that measurable crystallization begins on the same time scales as those of the solution temperature transients shown in Figure 1, and as will be shown, crystallization is nearly complete on the same time scales as those for late-stage coarsening of the liquid−liquid structures determined from light scattering.

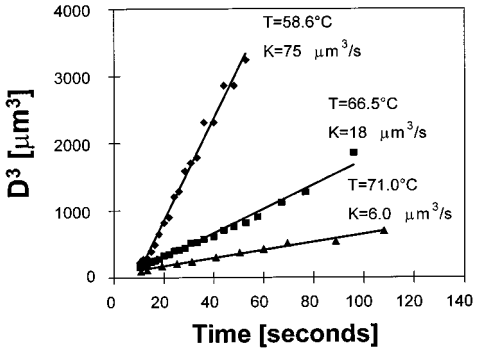

Figure 4. Domain growth kinetics for 10 wt % co-PE solutions quenched to three temperatures in region I of the phase diagram.

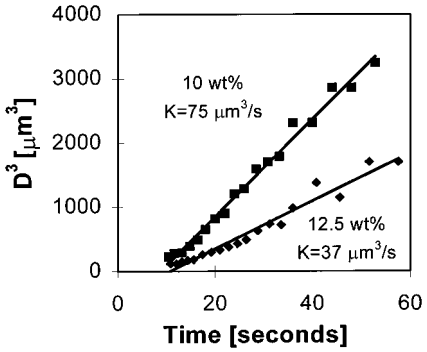

Figure 5. Domain growth kinetics for two concentrations quenched to 58.6 °C (Region I of phase diagram).

Phase Separation Kinetics. The time dependence of the position of the small angle light scattering maximum was used to quantify the dominant length scale in the phase-separating system, D. The latter can be directly related to the scattering vector, q_m ($=4n\pi/\lambda \sin(\theta_m/2)$, where θ_m is the angular position of the light scattering intensity maximum, λ is the wavelength in vacuo, and n is the solution refractive index), by[7,17,18,19]

$$D = \frac{2\pi}{q_m} \tag{1}$$

Analyses have shown that the kinetics remain relatively constant whether one bases them on the intensity maximum or the first moment of the distribution.[24] Numerical simulations of the late stages of spinodal decomposition[24] as well as several models for domain growth, including droplet coalescence[20] and Ostwald ripening,[21] predict that the domain size, D, should scale with $t^{1/3}$ or

$$D^3 = D_o^3 + K(t - t_o) \tag{2}$$

where D_o is the length scale at the end of the early stage time period, t_o, and K is the growth rate. Figures 4 and 5 illustrate how the growth rate, K, changes as the temperature and concentration are varied within region I of the phase diagram. In the first case, Figure 4, the

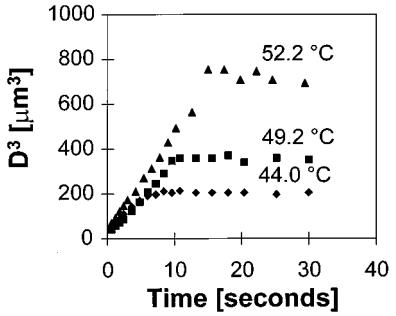

Figure 6. Domain growth kinetics for 10 wt % co-PE/anisole solutions quenched to three temperatures below the crystallization temperature (region III).

phase separation dynamics were monitored for a 10 wt % co-PE anisole solution at three temperatures progressively closer to the crystallization temperature. The linearity of the data at all three temperatures shows that the coarsening kinetics are well-described by a power law with a time exponent of one-third. Equally important is the fact that the growth rate, K, increases with increasing quench depth. While this is a commonly observed trend in phase separating polymer solutions,[10,22,23] it contrasts rather dramatically with the behavior of the atactic PMMA/cyclohexanol system,[7] described in our earlier study, where the growth rate sharply decreased with increasing quench depth. In the latter case, the quench temperatures were all close to the glass transition temperature. Our calculations, based on the Cahn−Hilliard formalism,[24] demonstrate that, in the region of a glass transition, the system mobility can dominate the kinetics, leading to a lowering of the growth rates at lower temperatures. As the glass transition temperature of the polyethylene copolymer used in this study is presumably quite low (T_g of PE $\sim$ −80 °C[25]), the present results represent a case where the increase in the thermodynamic driving force for coarsening clearly dominates the slight changes in transport kinetics that occur for systems far removed from the glass transition.[24]

In addition to the effect of quench temperature on the phase separation dynamics, small changes in the overall polymer concentration can result in relatively large changes in the growth rate. Figure 5 demonstrates that the coarsening kinetics at 58.6 °C decrease on changing the initial composition from 10 wt % to 12.5 wt %. A similar pattern has been observed in the coarsening kinetics of fractionated polystyrene solutions in cyclohexane and quantitatively interpreted in terms of a diffusive coarsening model.[26] Although our sample is polydisperse, this correspondence would suggest that a similar explanation may hold.

Figures 6−9 show how the confluence of liquid−liquid phase separation and crystallization affects the phase separation kinetics and final morphology. Figure 6 shows growth rate data for 10 wt % solutions which were quenched to three different temperatures in region III, below the crystallization line. One sees that the liquid−liquid phase separated structure coarsens for a brief period before being abruptly arrested by crystallization. The times in Figure 6 corresponding to the point at which structure locks in for each of the three temperatures are shown as dotted lines in Figure 1. From this we conclude that cessation of domain growth occurs when the solution temperatures reaches 55 °C, a value slightly higher than that shown of the phase

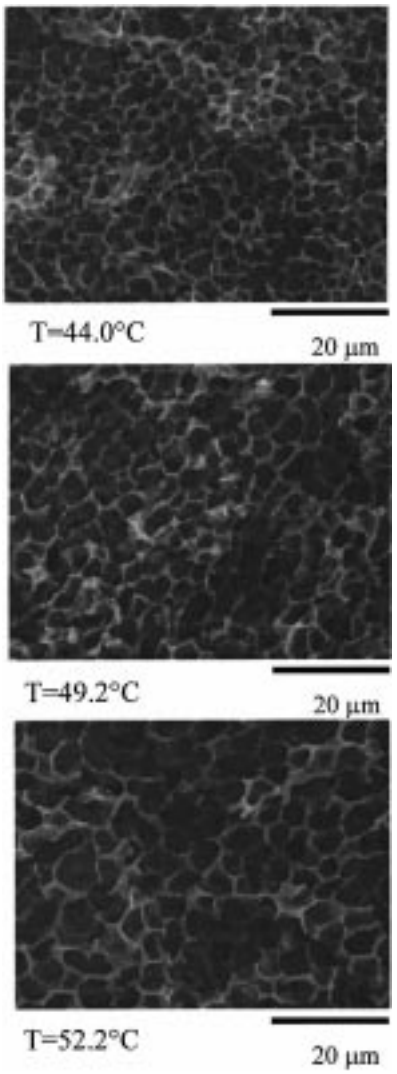

Figure 7. Morphologies of 10 wt % co-PE/anisole solutions quenched to the three temperatures shown in Figure 6.

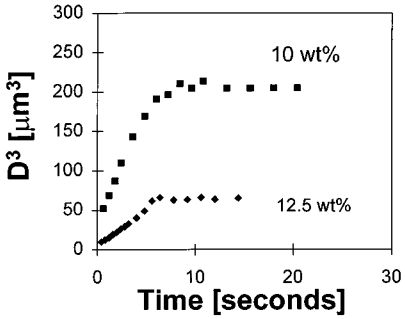

Figure 8. Domain growth kinetics for two concentrations quenched to 44.0 °C in region III.

diagram. The slight difference, we believe, reflects differences in the heat transfer characteristics of the two experiments. Nevertheless, these data clearly indicate that cessation of domain growth occurs essentially immediately once the solution temperature crosses the crystallization line. Thus, the decrease in final domain size with decreasing quench temperature results primarily from a decrease in the time spent in region I, rather than from the faster crystallization kinetics at the lower temperatures. Moreover, these data illustrate that changes in the processing that affect the time spent above the crystallization temperature will be directly

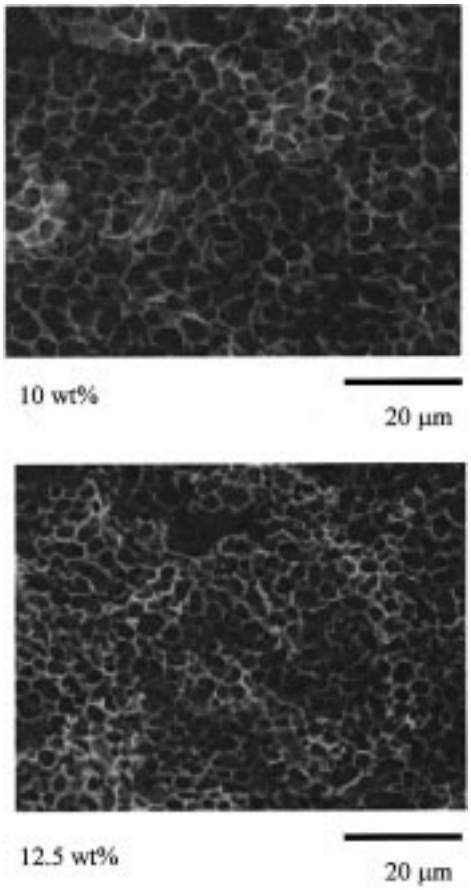

Figure 9. Morphologies of films that were quenched under the same conditions as Figure 8.

manifested as a change in the pore size of the final product. This is further shown in the SEM micrographs in Figure 7 of the samples prepared under the conditions given in Figure 6. The cellular morphologies are characteristic of liquid−liquid phase separation, indicating that crystallization locks in the structure rather than contributing new morphological characteristics. Figure 8 shows the evolution of structure for two concentrations quenched to region III, below the crystallization temperature. Comparison of these data to Figure 5 clearly suggests that, in regions above the crystallization temperature, the liquid phase growth rate decreases with increasing concentration. This is also evidenced in the smaller pore sizes at the higher concentration shown in Figure 9. These results clearly suggest that varying the overall polymer concentration can provide an effective means to control the pore size of membranes made from crystallizable solutions.

In summary this study demonstrates that crystallization is a viable mechanism for locking in the two-phase structure in thermal induced phase separation. Furthermore, the precise size scale one sees in the morphology will depend on the balance between the heat transfer kinetics during quenching and the growth kinetics of the two-phase structure. As such, these results suggest a way to predict and control the structure formation process.

Acknowledgment. This work has been supported under a grant from the National Science Foundation, CTS 94-21580. Some of the data in this paper were obtained by Mr. D. L. Fitzgerald and Mr. A. J. Pervan both of whom have been supported by a Hauser Scholarship in the Department of Chemical Engineering.

References and Notes

(1) Aubert, J. H.; Clough, R. L. *Polymer* **1985**, *26*, 2047.
(2) Castro, A. J. U.S. Patent 4 247 498, Jan 27, 1981.
(3) Caneba, G. T.; Soong, D. S. *Macromolecules* **1985**, *18*, 2538.
(4) Lloyd, D. R.; Kinzer, K. E.; Tseng, H. S. *J. Membr. Sci.* **1990**, *52*, 239.
(5) Lloyd, D. R.; Kin, S. S.; Kinzer, K. E. *J. Membr. Sci.* **1991**, *64*, 1.
(6) Bansil, R.; Lal, J.; Carvalho, B. L. *Polymer* **1992**, *33*, 2961.
(7) Graham, P. D.; Pervan, A. J.; McHugh, A. J. *Macromolecules* **1997**, *30*, 1651.
(8) Laxminarayan, A.; McGuire, K. S.; Kim, S. S.; Lloyd, D. R. *Polymer* **1994**, *35*, 3060.
(9) Zryd, J. L.; Burghardt, W. R. *J. Appl. Polym. Sci.* **1995**, *57*, 1525.
(10) McGuire, K. S.; Laxminarayan, A.; Lloyd, D. R. *Polymer* **1995**, *36*, 4951.
(11) Richards, R. B. *Trans. Faraday Soc.* **1946**, *42*, 10.
(12) Soenen, H.; Berghmans, H. *J. Polym. Sci., Polym. Phys. Ed.* **1996**, *34*, 241.
(13) Stoks, W.; Berghmans, H. *J. Polym. Sci., Polym. Phys. Ed.* **1991**, *29*, 609.
(14) Aerts, L.; Kunz, M.; Berghmans, H.; Koningsveld, R. *Makromol. Chem.* **1993**, *194*, 2697.
(15) Flory, P. J. *Principles of Polymer Chemistry*; Cornell University Press: Ithaca, NY, 1953.
(16) Lee, H. K.; Myeson, A. S.; Levon, K. *Macromolecules* **1992**, *25*, 4002.
(17) Guinier, A.*X-ray Diffraction*; W. H. Freeman and Company: San Francisco, CA, 1963.
(18) Hashimoto, T.; Sasaki, K.; Kawai, H. *Macromolecules* **1984**, *17*, 2812.
(19) Lauger, J.; Lay, R.; Maas, S.; Gronski, W. *Macromolecules* **1995**, *28*, 7010.
(20) Binder, K.; Stauffer, D. *Phys. Rev. Lett.* **1974**, *33*, 1006.
(21) Lifshitz, I. M.; Slyozov, V. V. J. *Phys. Chem. Solids* **1961**, *19*, 35.
(22) Song, S.-W.; Torkelson, J. M. *Macromolecules* **1994**, *27*, 6389.
(23) Song, S.-W.; Torkelson, J. M. *J. Membr. Sci.* **1995**, *98*, 209.
(24) Barton, B. F.; Graham, P. D.; McHugh, A. J. *Macromolecules* **1998**, *31*, 1672.
(25) Boyer, R. F. *Rubber Chem. Technol. (Rubber Rev.)* **1963**, *36*, 1303.
(26) Aubert, J. H. *Macromolecules* **1990**, *23*, 1446.

MA971056P